J Solid State Electrochem (2013) 17:1711–1716
DOI 10.1007/s10008-013-2022-6

ORIGINAL PAPER

Flower-like NiO microspheres prepared by facile method as supercapacitor electrodes

Qingfeng Wu · Yafei Liu · Zhonghua Hu

Received: 12 November 2012 / Revised: 26 January 2013 / Accepted: 28 January 2013 / Published online: 20 February 2013

Abstract Hierarchical flower-like NiO microsphere was successfully synthesized by a simple one-step template-free hydrothermal process, using L-lysine as precipitator and nickel sulfate as nickel source. The as-synthesized materials were characterized by X-ray diffraction, field emission scanning electron microscope, high-resolution transmission electron microscope, and the electrochemical workstation. The electrochemical results show that the flower-like NiO microspheres exhibit specific capacitance as large as 324 $F g^{-1}$ at the current density of 2 $A g^{-1}$ and the specific capacitance retention can maintain 83 % after 1,000 cycles at the current density of 20 $A g^{-1}$ in 6 M KOH.

Keywords Nickel oxide · Flower-like microspheres · Supercapacitor electrodes · Template-free

Introduction

As a new device of electrical energy storage, electrochemical capacitors (ECs, also called supercapacitors) possess special characteristics of high power density, long cycling serving life, and fast charge–discharge rate. According to the energy storage mechanism of ECs, and active materials utilized, supercapacitors can be classified as electrochemical double layer capacitors (EDLCs) and pseudocapacitors. The former works base on the electric double layers formed on the interface of electrolytic solution and electrode; the last works base on the fast and reversible redox reactions of electrolyte on the surface of the working electrode [1, 2]. Pseudocapacitive materials, such as transition metal oxides, are being explored for use in supercapacitors with a larger specific capacitance and higher energy density than EDLCs. RuO_2 [3, 4] is a super electrode material with a specific capacitance as high as 900 $F g^{-1}$, but ruthenium is a precious metal and has high cost, so it is difficult to adapt to the commercial application. Although other transition metal oxides, such as Co_3O_4 [5–7], NiO [8–10], and MnO_2 [11–13], are not better than RuO_2 when they were used as electrode material, they also have big specific capacitance and their costs are much lower than RuO_2. These metal oxides could be used as promising electrode materials for pseudocapacitors as substitutes for RuO_2 [9, 14]. In this case, researchers have made many efforts to improve their properties to adapt to the actual application.

NiO is a very important transition metal oxide with applications in lithium ion batteries, gas sensors, electrochromic devices, and supercapacitors owing to its availability, low cost, and rather good pseudocapacitive behavior. NiO electrode materials can be prepared with many kinds of morphology, such as nanosheet, nanoflower, and nanotube. Since the morphology, structure, and size of the materials have significant influence on the physical and chemical properties of NiO, the production of this kind of material with diverse morphology and self-assembled hierarchical structure has attracted enormous interest in materials science and industry [15–17].

In the present work, flower-like NiO microspheres were prepared by a facile method of hydrothermal process using $NiSO_4 \cdot 6H_2O$ as nickel source and L-lysine as precipitator in order to improve its morphology and enhance the electrochemical performance. Yuan et al. prepared Co_3O_4 with L-lysine [18] and their experiment results showed that the Co_3O_4 electrode material had excellent electrochemical

Q. Wu (✉) · Y. Liu · Z. Hu
Department of Chemistry, Tongji University, 1239 Siping Road, Shanghai 200092, People's Republic of China
e-mail: lanmozhilei_2008@126.com

properties. Through surveying a great number of literatures, we find that there was no report about using L-lysine to prepare NiO, so we did this work. The flower-like NiO microspheres synthetized by our method exhibit excellent pseudocapacitive performance with high rate discharge and high capacity retention, especially at high current densities.

Experimental

Synthesis of flower-like NiO microspheres

The flower-like NiO microspheres were prepared by a template-free hydrothermal method [18]. $NiSO_4 \cdot 6H_2O$ (1.3142 g; analytically pure, Sinopharm) and 1.4619 g L-lysine (analytically pure, Sinopharm) were dissolved in 60 ml of twice deionized water. The solution was magnetically stirred for 30 min in air at room temperature, and then the solution was transferred into a Teflon-lined stainless steel autoclave of 100 ml. The autoclave was sealed and maintained at 100 °C for 36 h in an electric oven. After cooled down to room temperature naturally, the precipitate was washed with twice deionized water and absolute ethyl alcohol several times. The precipitate was dried at 60 °C for 6 h in an electric oven and subsequently heated at 300 °C for 4 h in air at the rate of 1 °C min^{-1} to obtain the final product.

Prepare of NiO working electrode

The working electrode was prepared with the active material NiO, carbon black, and polytetrafluoroethylene at the weight ratio of 8:1:1. A small amount of absolute ethanol was added to this mixture and ultrasonic was used to scatter them evenly. After drying at 60 °C for several hours until the mixture becomes viscous, a small wafer was cut from the mixture with a hole puncher. Lastly, the small wafer was pressed onto a nickel grid with a surface area of 1 cm^2 at a pressure of 20 MPa. After all these procedures, you will get the working electrode.

Characterizations

The prepared sample was examined by X-ray diffraction (XRD; D8, Bruker), field emission scanning electron microscope (FESEM; XL30, Philips), and high-resolution transmission electron microscope (HRTEM; JEM-2100, JEOL). Electrochemical measurements were performed with an electrochemical cell of conventional three electrodes using electrochemical workstation (Chi660c, Chenhua). The NiO materials acted as working electrode, nickel grid was employed as counter electrode, and Hg/HgO electrode served as reference electrode. All the electrochemical measurements were performed in KOH aqueous solution of 6 mol L^{-1} at room temperature.

Results and discussion

Characterization of NiO

The structure of the NiO powder sample was studied by XRD and the corresponding XRD pattern is shown in Fig. 1a. The diffraction peaks are indexed at 2θ values of 37°, 43°, 63°, 75°, and 79°, which correspond to the (110), (200), (220), (311), and (222) reflections of NiO structures and all the peaks are perfectly in agreement with the standard spectrum of NiO (JCPDS, 47-1049). The relatively high peak intensities indicate that NiO are of high crystallinity and no other peaks of impurities are observed.

The surface morphology of the NiO microspheres at different resolution ratio was imaged by FESEM and is shown in Fig. 2a–d. It is clear that the NiO nanosheets are interlaced each other to form an ordered nano-grid structure with a kind of highly open and porous structure just like flower clusters (Fig. 2a). At a higher resolution ratio (Fig. 2b), we can find that the NiO microsphere is similar with a white rose. Interestingly, we do not only get the three-dimensional flower structure, but also the plane lamellar structure partly (Fig. 2c). This may because during the process of crystal growth, the NiO nanosheets encountered the bottom of the reactor, so they grow along the bottom plane to form a plane lamellar structure. Actually, the porous feature of the flower-like nickel

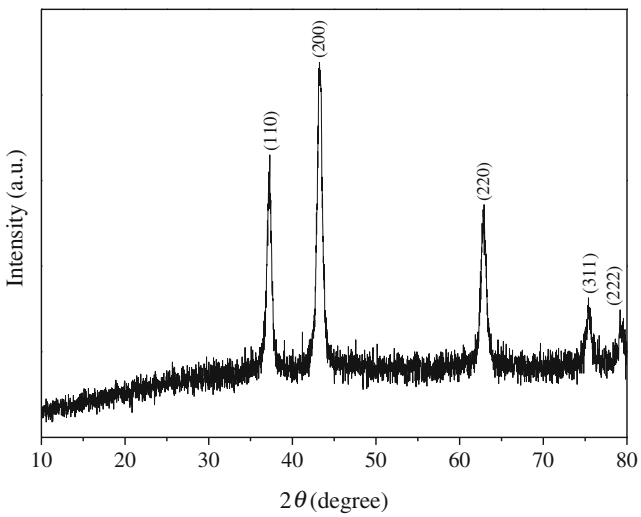

Fig. 1 XRD pattern of the NiO powder sample

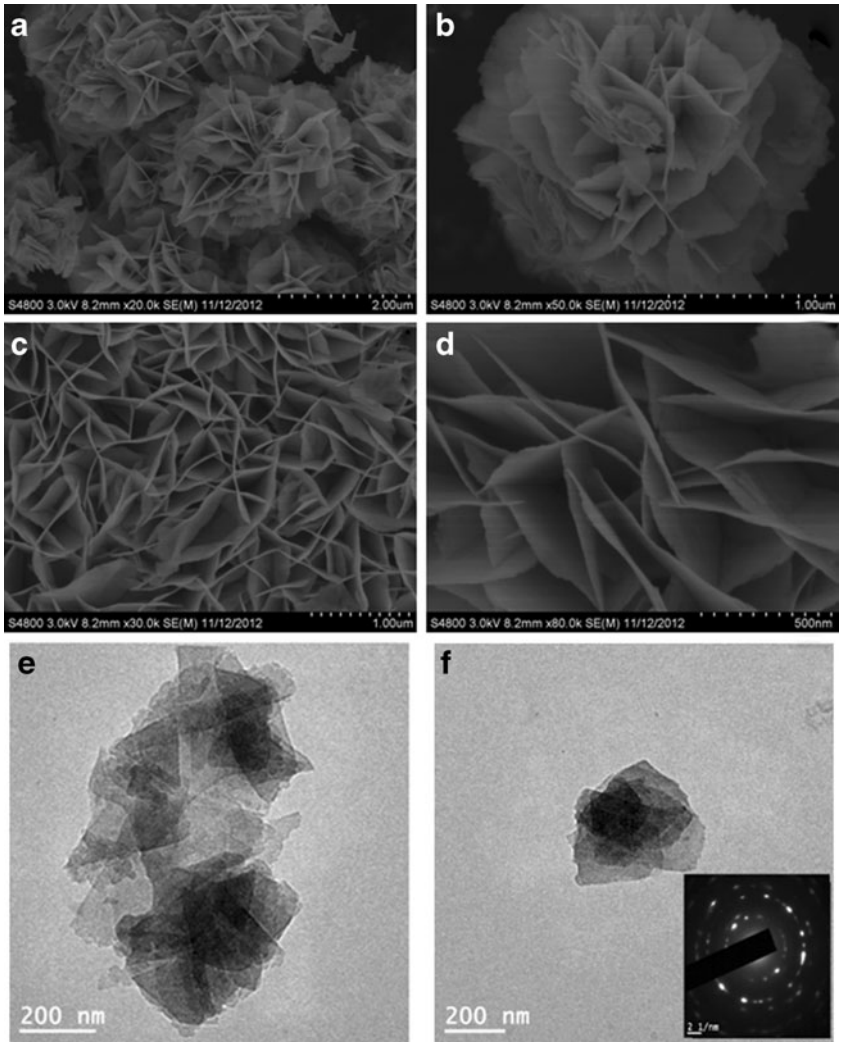

Fig. 2 **a**–**f** The FESEM and HRTEM images of the NiO powder sample at different resolution ratio

oxide can be confirmed by high-resolution FESEM image (Fig. 2d). The thickness of the petal is found to be approximately 10 nm.

For better understanding of dimensionality of the nanoflower morphologies, HRTEM was used. Figure 3e, f shows high magnification TEM images of NiO nanoflowers. From the images, we can see that the NiO nanoparticles are arranged orderly to form the nanoflower structure. It is clearly visible that the NiO nanoflowers are polycrystalline from the SAED pattern (inset in Fig. 3f), having a layered structure. This is consistent with the results from the SEM images and the diffraction rings match the XRD peaks very well.

In this work, L-lysine was used as a precipitant to form NiO nanoflower. It is a weak base and it released free OH^- ions much less than those of strong bases (such as NaOH and KOH) in the aqueous solution. The hydrolysis of L-lysine and the precipitation reaction are expressed as follows:

$$H_2N(CH_2)_4CH(NH_2)COOH + H_2O\left[H_3N(CH_2)_4CH(NH_2)COOH\right]^+ + OH^- \quad (1)$$

$$Ni^{2+} + 2OH^- \rightleftarrows Ni(OH)_2 \quad (2)$$

The low concentration and slow release of OH^- could effectively decrease the reaction rate of precipitation and prevent the growth of $Ni(OH)_2$ crystal, so that the formation of large particles can be avoided. The result suggested that L-lysine precipitant has an important influence on the $Ni(OH)_2$ precipitate formation. In the moment of the reaction, OH^- ions are relatively lacking, whereas Ni^{2+} cations

are exceeding, so that nanoscale $Ni(OH)_2$ precipitate can be produced. After heat treatment, the flower-like NiO microspheres were obtained.

Electrochemical properties of the NiO electrode

Reversible redox of NiO electrode

Cyclic voltammetry (CV) is a method used for the determination of the electrochemical properties of NiO electrodes. Figure 3 shows the cyclic voltammetry curves of the NiO electrode at different scan rates in 6 $molL^{-1}$ KOH aqueous solution. The scan rates were 5, 10, 20, and 40 mVs^{-1}. The shapes of the CV curves were different to those of the electric double layer capacitance, indicating that the two strong peaks correspond to the superficial faradic oxidation/reduction reactions. The oxidation peak at 0.47 V is due to the NiO conversion to NiOOH, whereas the reduction peak at 0.37 V is due to the reverse reaction. According to the redox mechanism, the faradic reaction is [19, 20]:

$$NiO + OH^- \rightleftarrows NiOOH + e^- \quad (3)$$

With the scan rate increased, the potential and the current at the two peaks shifted more towards the positive and negative axes, owing to the abundant surface area of the porous NiO and the fast ionic/electronic diffusion rate during the faradic redox reaction. In addition, the oxidation and reduction peaks are symmetrical throughout the whole range of scan rates, indicating good reversibility of redox reactions at/near the porous surfaces.

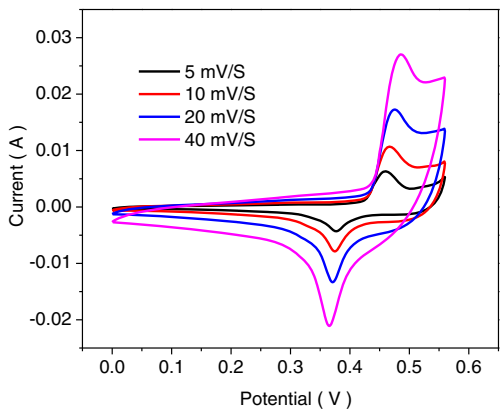

Fig. 3 CV curves at different sweep rates in 6 $molL^{-1}$ KOH electrolyte

Charge–discharge performance

The pseudo-capacitances of the NiO electrode are elucidated by galvanostatic charge–discharge tests in the potential range of 0 to 0.53 V (vs. Hg/HgO) at different galvanostatic current densities in 6 $molL^{-1}$ KOH aqueous solution and are shown in Fig. 4. The discharge branch usually consists of two regions, a sudden potential drop at the very beginning of discharge followed by a slow potential decay. The potential drop is caused by internal resistance of the electrode or capacitor device, and the subsequent potential decay is due to the continuous discharge.

It is clear that the NiO electrode has good capacitance features. The specific capacitance of the NiO nanostructures electrodes at the current density of 2 Ag^{-1} is calculated to be 324 Fg^{-1}. Importantly, at a high current density of 15 Ag^{-1}, the specific capacitance of the NiO nanostructure electrodes still remains at 251 Fg^{-1}. At other galvanostatic current density of 5, 10, and 30 Ag^{-1}, the corresponding specific capacitance is 300, 272, and 195 Fg^{-1}, respectively. The specific capacitance of the flower-like NiO microspheres is superior compared with previously reported values of other

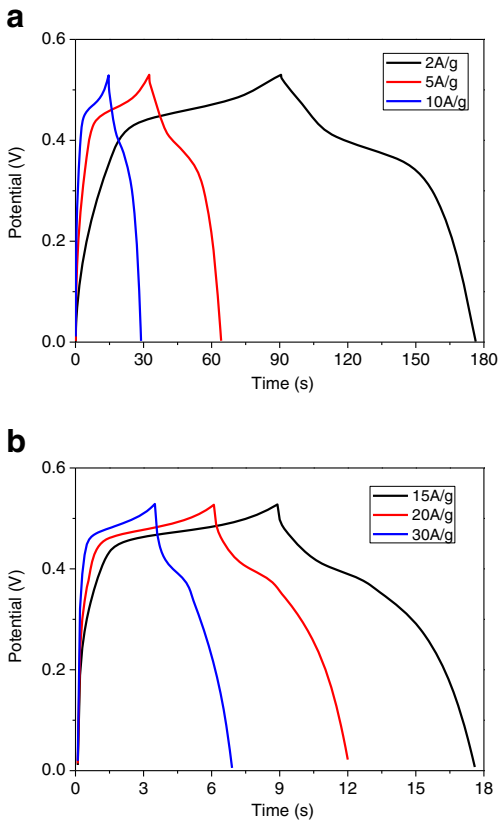

Fig. 4 **a**, **b** Galvanostatic charge–discharge curve at different current densities

NiO-based nanostructures [9, 21]. For example, the hierarchically porous NiO film synthesized by self-assembled method exhibits a specific capacitance of 232, 213, and 200 Fg^{-1} when the current density is 2, 10, and 20 Ag^{-1} [9]. In addition, the capacitance of the porous NiO nanowall array ordered structure obtained on conductive substrates is even lower than 250 Fg^{-1} at current density of 13.35 Ag^{-1} [21]. The value is higher than those of Co_3O_4 prepared by Li et al. (152 Fg^{-1} at the current density of 1.4 Ag^{-1}) [5] and the MnO_2 prepared by Yuan et al. (264 Fg^{-1} at the current density of 1.1 Ag^{-1}) [11].

Electrochemical impedance

The electrochemical impedance is also an important parameter, which directly affects the self-discharge efficiency of battery or capacitor. Figure 5 shows the Nyquist plots of the EIS spectra of the flower-like NiO electrode before (α) and after (β) a 1,000-cycle charge–discharge test at an open circuit potential. It is clear that at the high frequencies, both the inner resistances are very small (about 0.5 Ω) which is reflected by the intercept at real part (Z'). The inner resistance is a combination result of ionic resistance of electrolyte, intrinsic resistance of substrate, and contact resistance at the active material/current collector interface. The smaller the inner resistance, the less the self-discharge, the higher the coulomb efficiency, and the higher the power density ($P = V^2/4R$).

As shown in the inset of Fig. 5, it is hard to observe the semicircular arc in the high frequency region, indicating a low charge–transfer resistance (R_{ct}) caused by faradaic reactions, i.e., fast redox kinetics. In the low-frequency region, both straight lines incline at an angle much large than 45°, indeed nearly 90° to the Z'-axis, indicative of a low diffusive resistance of electrolyte in electrode.

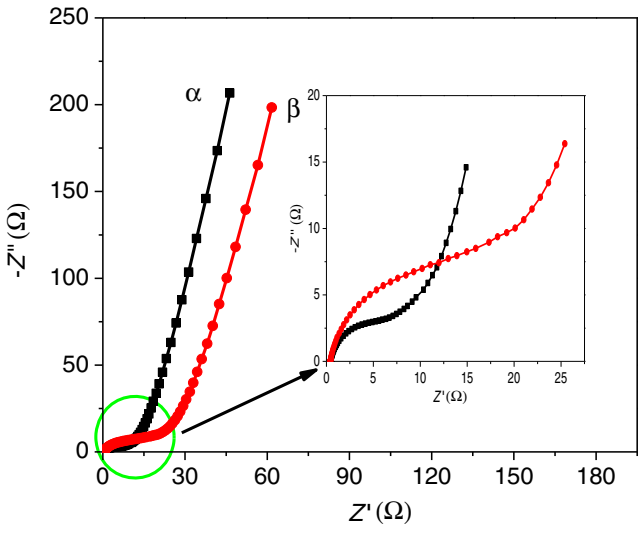

Fig. 5 Nyquist plots after a 1,000-cycle charge–discharge

Cyclic stability

The cyclic ability of electrode is an important parameter for the practical application. As shown in Fig. 6, after a 1,000-cycle charge–discharge test at the constant and high current of 20 Ag^{-1}, the specific capacitance reduces a little from original 234 to 189 Fg^{-1}; the capacitance retention is as high as 83 %, indicating that the flower-like NiO microspheres are very stable electrode material. The inset of Fig. 6 shows the last eight charge–discharge cycles of the NiO nanostructures.

Conclusions

The flower-like NiO microspheres were successfully prepared by a facile hydrothermal method. The main difference with other preparation methods reported in literature is that L-lysine was used as precipitator, which release OH^- during the hydrothermal process and influence the formation of Ni $(OH)_2$. It exhibits good electrochemical performance. The specific capacitance is as high as 324 Fg^{-1} at 2 Ag^{-1}; even at very high current density of 20 Ag^{-1}, the capacitance could reach to 234 Fg^{-1}. The capacitance retention could be 83 % after a 1,000-cycle of charge–discharge test. This work demonstrates that the flower-like NiO is a promising electrode material with large capacitance, high power, and high stability for electrochemical capacitor, especially at high current densities.

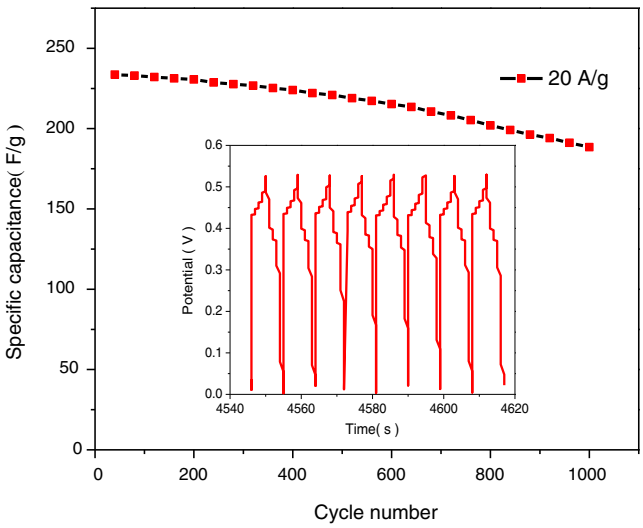

Fig. 6 A 1,000-cycle charge–discharge test at the current density of 20 Ag^{-1}

Acknowledgments This work was supported by Tongji University Research Foundation (1380219039). The authors would like to thank the colleagues from the Chemistry Experimentation Center of Tongji University for their help in the sample characterization.

References

1. Simon P, Gogotsi Y (2008) Nat Mater 7:845
2. Zhang Y, Feng H, Wu XB (2009) Int J Hydrog Energy 34:4889–4899
3. Takasu Y, Arikawa T, Yanase K (1997) J Alloys Comp 261:172–175
4. Su YF, Wu F, Bao LY, Yang ZH (2007) New Carbon Mater 22:53–57
5. Li YH, Huang KL, Yao ZF, Liu SQ, Qing XX (2011) Electrochim Acta 56:2140–2144
6. Kim YS, Yi CW, Choi HS, Kim K (2011) J Power Sources 196:1886–1893
7. Zhang P, Guo ZP, Huang YD, Jia DZ, Liu HK (2011) J Power Sources 196:6987–6991
8. Huang XH, Tu JP, Xia XH, Wang XL, Xiang JY, Zhang L (2010) J Power Sources 195:1207–1210
9. Zhang YQ, Xia XH, Tu JP, Mai YJ, Shi SH, Wang XL, Gu CD (2012) J Power Sources 199:413–417
10. Mai YJ, Shi SJ, Zhang D, Lu Y, Gu CD, Tu CD (2012) J Power Sources 204:155–161
11. Yuan CZ, Gao B, Su LH, Zhang XG (2008) J Colloid Interf Sci 322:545–550
12. Lei Y, Daffos B, Taberna PL, Simonb P, Faviera F (2010) Electrochim Acta 55:7454–7459
13. Fan Z, Chen JH, Zhang B, Liu B, Zhong XX, Kuang YF (2008) Diam Relat Mater 17:1943–1948
14. Chen J, Xia XH, Tu JP, Xiong QQ, Yu YX, Wang XL, Gu CD (2012) J Mater Chem 22:15056–15061
15. Lang JW, Kong LB, Wu WJ, Luo YC, Kang L (2008) Chem Commun 18:4213–4215
16. Mai YJ, Tu JP, Gu CD, Wang XL (2012) J Power Sources 209:1–6
17. Needham SA, Wang GX, Liu HK, Drozd VA, Liu RS (2007) J Power Sources 174:828–831
18. Yuan CZ, Zhang XG, Hou LR, Shen LF, Li DK, Zhang F, Fan CG, Li JM (2010) J Mater Chem 20:10809–10816
19. Xia XH, Tu JP, Zhang J, Wang XL, Zhang WK, Huang H (2008) Sol Energy Mater Sol Cells 92:628–633
20. Chigane M, Ishikawa M (2000) J Electrochem Soc 147:2246–2251
21. Zhu JH, Jiang J, Liu JP, Ding RM, Ding H, Feng YM, Wei GM, Huang XT (2011) J Solid State Chem 184:578–583